



2006

Bound States in the Continuum in Quantum-Dot Pairs

Gonzalo Ordonez

Butler University, gordonez@butler.edu

Kyungsun Na

Sungyun Kim

Follow this and additional works at: https://digitalcommons.butler.edu/facsch_papers



Part of the [Quantum Physics Commons](#)

Recommended Citation

Ordonez, Gonzalo; Na, Kyungsun; and Kim, Sungyun, "Bound States in the Continuum in Quantum-Dot Pairs" *Physical Review A* / (2006): -.

Available at https://digitalcommons.butler.edu/facsch_papers/727

This Article is brought to you for free and open access by the College of Liberal Arts & Sciences at Digital Commons @ Butler University. It has been accepted for inclusion in Scholarship and Professional Work - LAS by an authorized administrator of Digital Commons @ Butler University. For more information, please contact digitalscholarship@butler.edu.

Bound states in the continuum in quantum-dot pairs

Gonzalo Ordóñez* and Kyungsun Na

Center for Studies in Statistical Mechanics and Complex Systems, The University of Texas at Austin, Austin, Texas 78712, USA

Sungyun Kim

Max-Planck Institute for Physics of Complex Systems, Noethnitzer Str. 38, 01187 Dresden, Germany

(Received 20 April 2005; published 17 February 2006)

It is shown that for two open quantum dots connected by a wire, “bound states in the continuum” of a single electron are formed at nearly periodic distances between the dots. This is due to Fabry-Pérot interference between quasibound states in each dot. The bound states are nonlocal, describing the electron trapped in both dots at the same time. Theoretical and numerical results show that trapped states exist even if the wire connecting the dots is relatively long.

DOI: 10.1103/PhysRevA.73.022113

PACS number(s): 03.65.-w, 73.23.-b, 73.63.-b

Ever since von Neumann and Wigner [1] proposed that a certain type of oscillating attractive potentials could produce isolated bound states with energies within the continuum [2], a number of studies have reported the existence of “bound states in the continuum” (BIC) that can exist above the continuum minimum. Fonda and Newton discussed BIC in a system of two coupled square-well potentials using resonance scattering theory [3]. Friedrich and Wintgen found BIC in systems of coupled Coulombic channels, such as the hydrogen atom in a uniform magnetic field [4]. Positive-energy bound states in superlattice structures with a single impurity potential [5] or a single defect stub [6] have been reported.

The existence of BIC has been theoretically demonstrated as well in a pair of quantum dots coupled to reservoirs [7,8]. The pair of dots is regarded as a “molecule” with discrete energy levels. As far as we know, until now there has been no experimental realization of BIC in quantum dots.

Here we consider a quantum-dot system where the dots are two-dimensional square cavities connected to a lead as shown in Fig. 1. We show both theoretically and numerically that BIC can appear due to Fabry-Pérot interference between the quasibound states of each dot. The BIC appear at nearly periodic distances between the dots. In contrast to Refs. [7,8], instead of one “molecule” we have two separate dots that can be far apart. Therefore we study quite a different regime of electron transport between dots.

The dots and lead are a two-dimensional electron waveguide, which can be formed at a GaAs/(Al,Ga)As interface [9]. Electron waveguides may be formed as well using carbon nanotubes, where Fabry-Pérot interference for electron wave functions has been demonstrated experimentally [10]. In this Rapid communication we will focus on semiconductor waveguides. Our analysis can be easily extended to nanotubes.

The lead in Fig. 1 is an infinite quasi-one-dimensional wire, where electrons have a continuous spectrum of energy.

Due to the lateral confinement in the wire, the spectrum has a minimum energy that allows propagation along the wire. If there is a single dot, an electron inside the dot with energy below the minimum will be in a bound state. In contrast, an electron with energy above the minimum will be in a quasibound state with finite lifetime, eventually escaping the dot through the leads. Bound states and quasibound state are associated with real and complex poles of the S matrix [11], respectively. For the double dot, the electron states are much more varied. In this study, we focus on the interplay between the quasibound states formed in each dot.

Theoretical model. We consider the single-electron Hamiltonian

$$H = -\frac{\hbar^2}{2m_e^*} \left(\frac{\partial^2}{\partial x^2} + \frac{\partial^2}{\partial y^2} \right), \quad (1)$$

with vanishing wave functions at the boundaries. The effective mass is $m_e^* = 0.05m_e$, where m_e is the mass of the free electron. We assume the two dots are identical. To analyze this Hamiltonian, we decompose the system into two independent closed dots and the lead [14]. The wave functions inside the dots are denoted by $|m, n\rangle_i$, where $i=1, 2$ labels the dots and m, n are positive integers representing the horizontal and vertical wave numbers. The wave functions in the leads are denoted by $|k, j\rangle$ where k is the horizontal wave number (real) and j the vertical wave number (positive integer). The energies of the wave functions in either dot and the lead are, respectively,

$$E_d(m, n) = \frac{\hbar^2}{2m_e^*} \left[\left(\frac{m\pi}{L_d} \right)^2 + \left(\frac{n\pi}{W_d} \right)^2 \right],$$

$$E_l(k, j) = \frac{\hbar^2}{2m_e^*} \left[k^2 + \left(\frac{j\pi}{W_l} \right)^2 \right]. \quad (2)$$

The minimum energy for propagation along the lead is $E_l(0, 1)$. We consider an electron with low energy narrowly centered around $E_d^0 = E_d(m_0, n_0)$. We assume that $E_l(0, 1) < E_d^0 < E_l(0, 2)$. The electron may propagate through the first mode of the lead, but not through the higher ($j > 1$) modes.

*Current address: Physics and Astronomy Department, Butler University, Indianapolis, IN 46208, USA.

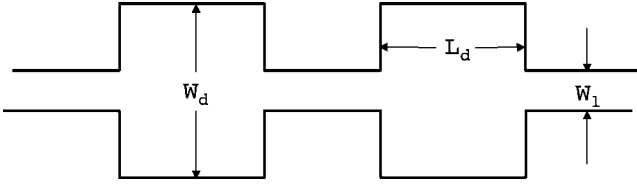


FIG. 1. Quantum-dot pair.

In our theoretical model, we neglect the $j > 1$ modes, which are evanescent, and keep only the $j = 1$ mode. Henceforth we omit the $j = 1$ index—e.g., $E_l(k) = E_l(k, 1)$.

We will rewrite the Hamiltonian using the dot and lead basis states. With $|i\rangle = |m_0, n_0\rangle_i$, we define the dot and lead projectors

$$P_d = \sum_{i=1}^2 |i\rangle\langle i|, \quad P_l = \int_{-\infty}^{\infty} dk |k\rangle\langle k|. \quad (3)$$

To make the basis states orthogonal, we introduce the modified lead states

$$|\psi_k\rangle = |k\rangle - RP_d(P_dRP_d)^{-1}|k\rangle, \quad (4)$$

$$R = \frac{1}{E_l(k) - P_lHP_l + i0},$$

which satisfy $\langle i|\psi_k\rangle = 0$ and $\langle\psi_{k'}|H|\psi_k\rangle = E_l(k)\delta(k-k')$. The following approximate Hamiltonian is obtained:

$$H \approx E_d^0[|1\rangle\langle 1| + |2\rangle\langle 2|] + \int_{-\infty}^{\infty} dk E_l(k) |\psi_k\rangle\langle\psi_k| + \left[\int_{-\infty}^{\infty} dk \sum_{i=1}^2 V_i(k) |i\rangle\langle\psi_k| + \text{H.c.} \right]. \quad (5)$$

The terms $V_i(k) = \langle i|H|\psi_k\rangle$ represent the amplitude of a transition of the electron from the lead to the dots or vice versa. For dots centered at $x = x_1$ and $x = x_2$, they have the form

$$V_{1,2}(k) = v_k e^{ikx_{1,2}} + u_k e^{ikx_{2,1}}. \quad (6)$$

We will construct eigenstates of the Hamiltonian (5) following Ref. [12], where the appearance of BIC for a one-dimensional two-atom system with a Hamiltonian similar to (5) was considered (see also [13]). We start with the symmetric and antisymmetric states

$$|\pm\rangle = (|1\rangle \pm |2\rangle)/\sqrt{2}, \quad (7)$$

which are unperturbed degenerate eigenstates of two closed cavities. Using these states as a basis, we build perturbed eigenstates of H . The eigenstates retain the symmetry of the corresponding unperturbed states (7), but they are no longer degenerate. In fact, they have complex energy eigenvalues z_{\pm} [12], which are poles of the S matrix. The eigenstates decay exponentially for $t > 0$ [with $\text{Im}(z_{\pm}) < 0$]. The eigenvalues are solutions of the integral equation

$$z_{\pm} = E_d^0 + 2 \int_0^{\infty} dk \frac{|u_k \pm v_k|^2}{[z_{\pm} - E_l(k)]^+} (1 \pm \cos kd) \quad (8)$$

closest to the real axis. Here $d = |x_2 - x_1|$ is the distance between the dots. The + superscript means analytic continuation from the upper to the lower half-plane of z_{\pm} . As the distance d is varied, the poles z_{\pm} move in the complex plane. At certain distances d_{\pm} the imaginary part of z_{\pm} vanishes [12]. This happens when $1 \pm \cos kd_{\pm} = 0$ for $E_l(k) = z_{\pm}$. These conditions give

$$d_{\pm} = \frac{2n + (1 \pm 1)/2}{\sqrt{2m_e^*[z_{\pm} - E_l(0)]}} \pi \hbar, \quad (9)$$

with n integer. Replacing $d = d_{\pm}$ in Eq. (8) we obtain the real solutions for z_{\pm} , which correspond to BIC. The appearance of BIC is essentially due to Fabry-Perot destructive interference between the wave functions escaping from each dot. This interference can only occur in a one-dimensional continuum (the quantum wire).

As shown in Ref. [12], BIC appear even for large d_{\pm} . Thus, in principle, the wire connecting the dots can be relatively long and still allow BIC. Note that d_{\pm} is a nonlinear function of n . Strictly speaking the distances d_{\pm} are not regularly spaced.

Computational results. We have computed the energy eigenstates for the lowest propagating mode in the double-dot waveguide as a function of energy and the distance between the two dots using the boundary integral method [11,15]. The eigenstates are built out of local propagating and evanescent modes in the leads and dots and are composed of incoming, $\psi^-(x, y)$, and outgoing, $\psi^+(x, y)$, states:

$$\psi(x, y) = \psi^-(x, y) + S(E)\psi^+(x, y), \quad (10)$$

where the scattering amplitude $S(E)$ is composed of reflection and transmission coefficients. As unit of length we take the width of the lead, $W_l = 1$, corresponding to 100 Å. As a

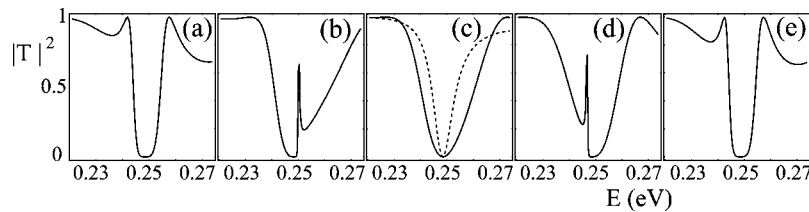


FIG. 2. Transmission probability $|T|^2$ versus energy E for the double-dot waveguide with (a) $d = 5.25$, (b) $d = 5.5$, (c) $d = 5.60$, (d) $d = 5.70$, and (e) $d = 5.90$. In this and the following figures the unit of length is 100 Å, and we have $W_d = 2$, $L_d = 2$, and $W_l = 1$. The dashed line in (c) is the transmission probability for the single-dot waveguide.

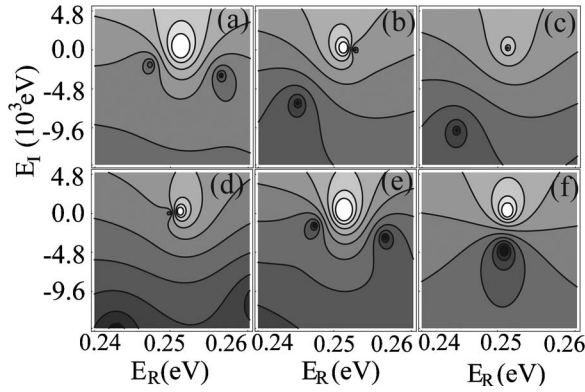


FIG. 3. Transmission amplitude $T(E)$ in the complex energy plane $E = E_R + iE_I$ for the double-dot waveguide with (a) $d = 5.25$, (b) $d = 5.5$, (c) $d = 5.60$, (d) $d = 5.70$, and (e) $d = 5.90$. The transmission amplitude in the complex energy plane for the single-dot waveguide is in (f). The dark regions indicate the positions of the poles, and the bright regions indicate the position of the transmission zero.

specific example, in this unit, we set the width and length of each dot to $W_d = 2$ and $L_d = 2$, respectively. These parameters satisfy the conditions of validity of the theoretical model.

We have computed the transmission probability $|T|^2$ for the lowest propagating mode as a function of energy for the double-dot waveguide in Fig. 2. As we vary the distance between the two dots, the transmission profiles change near the resonance energy region $E_d^0 = 0.25$ eV. This resonance corresponds to the energy of the $m_0 = 2$ and $n_0 = 3$ cavity mode in either dot. For the chosen parameters, this mode fulfills the condition $E_I(0, 1) < E_d^0 < E_I(0, 2)$ used in the theoretical analysis.

As shown in Figs. 2(b) and 2(d), there are sharp peaks in the transmission profiles on either side of the resonance energy region. In Fig. 2(c) we see a broad transmission profile with $d = 5.60$. For comparison, the transmission probability for the single-dot waveguide is shown in Fig. 2(c) as a dotted line. The transmission zero profile shows a wider dip for the double-dot waveguide as compared with that of the single-dot waveguide. We will see later that BIC is formed when $d = 5.60$, as well as at other values d that are nearly regularly spaced. These features are associated with the presence of two poles in the complex energy plane, which affect the dynamics of the electron in the double-dot waveguide.

The transmission zeros in Fig. 2 are associated with the poles of $T(E)$ in the complex energy plane. The transmission amplitude in the complex energy plane has a branch cut starting from the lower edge of the continuum and extending along the positive-energy axis and has poles at energies $z = \omega - i\gamma$. These poles give rise to the transmission zeros on the positive real axis [11,16].

The locations of the poles in the complex energy plane for the double-dot waveguide are shown in Fig. 3. As we in-

crease the distance between the two dots, the pole located on the right-hand side in Fig. 3(a) approaches the real axis. The pole disappears into the real axis and produces a zero value of γ at the distance, $d = 5.60$ in Fig. 3(c). This implies the formation of a BIC with infinite lifetime. The pole on the left-hand side in Fig. 3(a) moves away from the real axis and attains a large decay rate γ , accordingly. As the distance between the dots is further increased, the pole on the real axis in Fig. 3(c) emerges out of the transmission zero and recedes from the real axis [Fig. 3(d)]. If we continue to increase d , the pole on the right-hand side in Fig. 3(e) approaches the real axis and makes a transit through the transmission zero at $d = 6.28$ (not shown).

The wave functions inside the two dots associated with the right-hand-side and left-hand-side poles in Fig. 3(a) are, respectively, symmetric and antisymmetric with respect to cavity exchange. These wave functions are close to the symmetric and antisymmetric combinations of the eigenstates of the two closed dots with $m_0 = 2$ and $n_0 = 3$,

$$\psi_{\pm}(x, y) = \frac{1}{\sqrt{2}} \{ \sin[2\pi(x - x_1)/L_d] \cos(3\pi y/W_d) \chi_1 \pm \sin[2\pi(x - x_2)/L_d] \cos(3\pi y/W_d) \chi_2 \}, \quad (11)$$

where $\chi_i = 1$ inside dot i and $\chi_i = 0$ outside. Equation (11) corresponds to Eq. (7). The wave functions associated with each complex pole keep their symmetry or antisymmetry as the poles migrate throughout the complex energy plane, as we vary the distance between the two dots. The BIC appearing at $d = 5.6$ is symmetric and at $d = 6.28$ antisymmetric.

BIC reappear in a nearly periodic fashion as the distance between the two dots is varied (see Table I). This agrees with the existence of real solutions of Eq. (8) with Eq. (9) for different value of n . For example, the solution of Eq. (8) for $n = 4$ and $n = 5$ give $d_+ = 6$ and $d_- = 6.67$, respectively. The difference between the theoretical and computational values of d in Table I is likely due to the cutoff of $j > 1$ modes in the theoretical model [14]. However, the theoretical spacing between consecutive distances is in good agreement with the computational results. We have found, computationally, BIC for distances of up to $d \approx 50$, which means that these states may be quite delocalized.

In Fig. 3 each of the poles with either symmetric or antisymmetric identity makes a counterclockwise circulation that passes through the transmission zero on the real axis as vary the distance between dots. It has been known that the double or multiple poles induced by a laser in an atom coalesce to form an exceptional point or repel each other to form an avoided crossing [17–19]. In contrast, the poles of the double-dot waveguide make a circular motion and do not approach or repel each other.

The survival probabilities of an electron placed in the waveguide dots can be calculated using the scattering states

TABLE I. Computational (c) and theoretical (t) values of the interdot distance at which BIC appear.

$d(c)$	2.30	2.96	3.61	4.28	4.95	5.60	6.28	...	47.9	48.5	49.2
$d(t)$	2.67	3.33	4.00	4.67	5.33	6.00	6.67	...	48.7	49.3	50.0

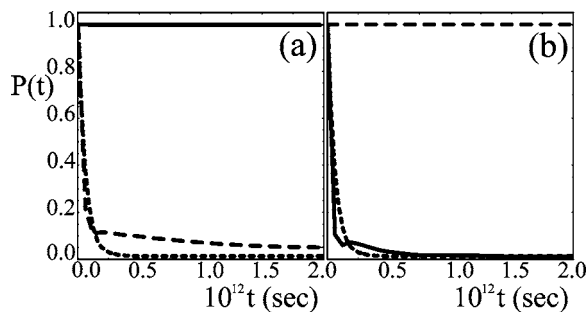


FIG. 4. The survival probability $P(t)=|A(t)|^2$ versus time t for the states prepared symmetrically or antisymmetrically inside the two dots at $t=0$. The distances between the two dots are (a) $d=5.60$ and (b) $d=6.28$. The dotted line shows the survival probability of a state in the single-dot waveguide in (a) and (b). The solid line displays the survival probability of a state prepared symmetrically, and the dashed line displays the survival probability of a state prepared antisymmetrically.

of the double-dot waveguide. The survival probability can be written as $P_\psi(t)=|A_\psi(t)|^2$, where $A_\psi(t)$ is the survival amplitude,

$$A_\psi(t) = \langle \psi | e^{-i\hat{H}t/\hbar} | \psi \rangle = \int_0^\infty dE |\langle \psi | E \rangle|^2 e^{-iEt/\hbar}. \quad (12)$$

We choose as initial state $|\psi\rangle$, the symmetric or antisymmetric combinations of the eigenstates of the two closed dots in Eq. (11), with no probability amplitude outside the dots. In order to solve Eq. (12) numerically we discretize the energy eigenstates $|E\rangle$ residing in the continuum. In Fig. 4, we plot the survival probability $P(t)=|A(t)|^2$ versus time t for the states prepared symmetrically or antisymmetrically inside the two dots at $t=0$. The distances between the two dots are $d=5.60$ and $d=6.28$ for Figs. 4(a) and 4(b), respectively.

With this arrangement, one of the complex poles has a vanishing imaginary part $\gamma \rightarrow 0$ and gives rise to an infinite lifetime. The results show that the symmetric (antisymmet-

ric) state does not decay over time for the cases with $d=5.60$ (6.28). On the other hand, the antisymmetric (symmetric) state decays quickly. The dotted line in Fig. 4 shows the survival probability of the state, $\psi = \sin(2\pi x/L_d)\cos(3\pi y/W_d)$, in the single-dot waveguide.

In conclusion, we have proved that there can be BIC in double-dot electron waveguides with specially arranged geometry. We could make the electron flow or get trapped inside the dots by controlling the size of one of the dots. This feature might be useful in a circuit device.

In both our theoretical and numerical analysis we have not discussed the Coulomb repulsion between electrons, because we considered single-electron states. Therefore we have no intradot or interdot Coulomb repulsion. One could consider electron pairs with opposite spins, though, with one electron placed within each dot. In this case BIC with large interdot distances as described in this paper could still appear, because for large interdot separations the Coulomb repulsion may be negligible. It is interesting to investigate the possibility of using such BIC to form delocalized, entangled states.

The existence of BIC may be verified experimentally using actual electron waveguides. Alternative experimental setups are electromagnetic waveguides, which are described by a similar model, and superlattices with two impurities [20]. Three-dimensional electron waveguides analogous to Fig. 1 may be constructed using nanotubes [10].

We have become aware that BIC in electron waveguides with a finite-size attractive impurity has been reported in Ref. [21]

We thank Professor T. Petrosky, Professor L. Reichl, Professor S. Tanaka, Professor R. Walser, and Professor P. Valanju for helpful comments and suggestions. We acknowledge the Engineering Research Program of the Office of Basic Energy Sciences at the U.S. Department of Energy, Grant No. DE-FG03-94ER14465 and U.S. Navy Office of Naval Research, Grant No. N00014-03-1-0639 for partial support of this work.

-
- [1] J. von Neumann and E. Wigner, *Phys. Z.* **30**, 465 (1929).
 [2] F. H. Stillinger and D. R. Herrick, *Phys. Rev. A* **11**, 446 (1975); B. Gazdy, *Phys. Lett.* **61A**, 89 (1977).
 [3] L. Fonda and R. G. Newton, *Ann. Phys. (N.Y.)* **10**, 490 (1960).
 [4] H. Friedrich and D. Wintgen, *Phys. Rev. A* **31**, 3964 (1985).
 [5] F. Capasso *et al.*, *Nature (London)* **358**, 565 (1992).
 [6] P. S. Deo and A. M. Jayannavar, *Phys. Rev. B* **50**, 11629 (1994).
 [7] M. L. Ladrón de Guevara, F. Claro, and P. A. Orellana, *Phys. Rev. B* **67**, 195335 (2003).
 [8] I. Rotter and A. F. Sadreev, *Phys. Rev. E* **71**, 046204 (2005).
 [9] S. Datta, *Electronic Transport in Mesoscopic Systems* (Cambridge University Press, Cambridge, England, 1995).
 [10] W. Liang *et al.*, *Nature (London)* **411**, 665 (2001); C. White and T. Todorov, *ibid.* **411**, 649 (2001).
 [11] K. Na and L. E. Reichl, *J. Stat. Phys.* **92**, 519 (1998).
 [12] G. Ordonez and S. Kim, *Phys. Rev. A* **70**, 032702 (2004).
 [13] G. Sudarshan, in *Field Theory, Quantization and Statistical Physics*, edited by E. Tirapegui (Reidel, Dordrecht, 1981), p. 237.
 [14] T. Petrosky and S. Subbiah, *Physica E (Amsterdam)* **19**, 230 (2003); S. Subbiah, Ph.D. Thesis, The University of Texas at Austin, 2000.
 [15] F. R. Frohne, M. J. McLennan, and S. Datta, *J. Appl. Phys.* **66**, 2699 (1989).
 [16] K. Na and L. E. Reichl, *Phys. Rev. B* **59**, 13073 (1999).
 [17] O. Latinne *et al.*, *Phys. Rev. Lett.* **74**, 46 (1995).
 [18] N. J. Kylstra and C. J. Joachain, *Phys. Rev. A* **57**, 412 (1998).
 [19] A. I. Magunov, I. Rotter, and S. I. Strakhova, *J. Phys. B* **34**, 29 (2001).
 [20] G. Ordonez, S. Tanaka, and T. Petrosky (unpublished).
 [21] C. S. Kim *et al.*, *Phys. Rev. B* **60**, 10962 (1999).